

## Hydrochemical Evaluation of the Miocene-Pliocene Aquifer System in Northern Saudi Arabia

ABDULAZIZ M. AL-BASSAM

*Dept. of Geology, College of Science,  
King Saud University, Riyadh, Saudi Arabia*

Received: 20/3/2004      Revised: 12/7/2004      Accepted: 18/7/2004

**ABSTRACT.** The Miocene-Pliocene aquifer system in northern Saudi Arabia represents an important groundwater resource. Groundwater occurs in multilayer water-bearing horizons of sandstone, chalk and marl. It moves under an average hydraulic gradient of 0.002 towards Sabkhat Hazouza. The average transmissivity is 20-170 m<sup>-2</sup>/day and the average storativity varies between  $0.11 \times 10^{-2}$  to  $3.7 \times 10^{-2}$ . The total mineralization of groundwater ranges from 430 to 6000 mg/l. The main water types is NaCl, with Ca-Mg-SO<sub>4</sub> as next in abundance. The main hydrochemical processes responsible for the water quality variations are ion-exchange, dissolution or mixing and limited reverse ion-exchange. The spatial distribution of the major ions, dissolved silica and iron are independent of the Sabkhat Hazouza. The salt effects of which seem to be restricted to the few meters close to the ground surface.

**KEYWORDS:** Miocene-Pliocene, Hydrochemical Evaluation, Northern Arabia.

### **Introduction**

The Miocene-Pliocene deposits form an important aquifer system in northern Saudi Arabia. It supplies water of variable quality in an area that is typically hyper arid. The study area lies between latitudes 29°30'-31°30' and longitudes 37°00'-39°00' (Fig. 1) it covers a surface area of about 110 km<sup>2</sup> of northern Saudi Arabia towards the borders with Jordan. It occupies most of the famous Wadi As Sirhan. Ground surface elevation reaches some 780 metres above mean sea level (a.m.s.l.) towards the northeast corner of the study area. It slopes down in

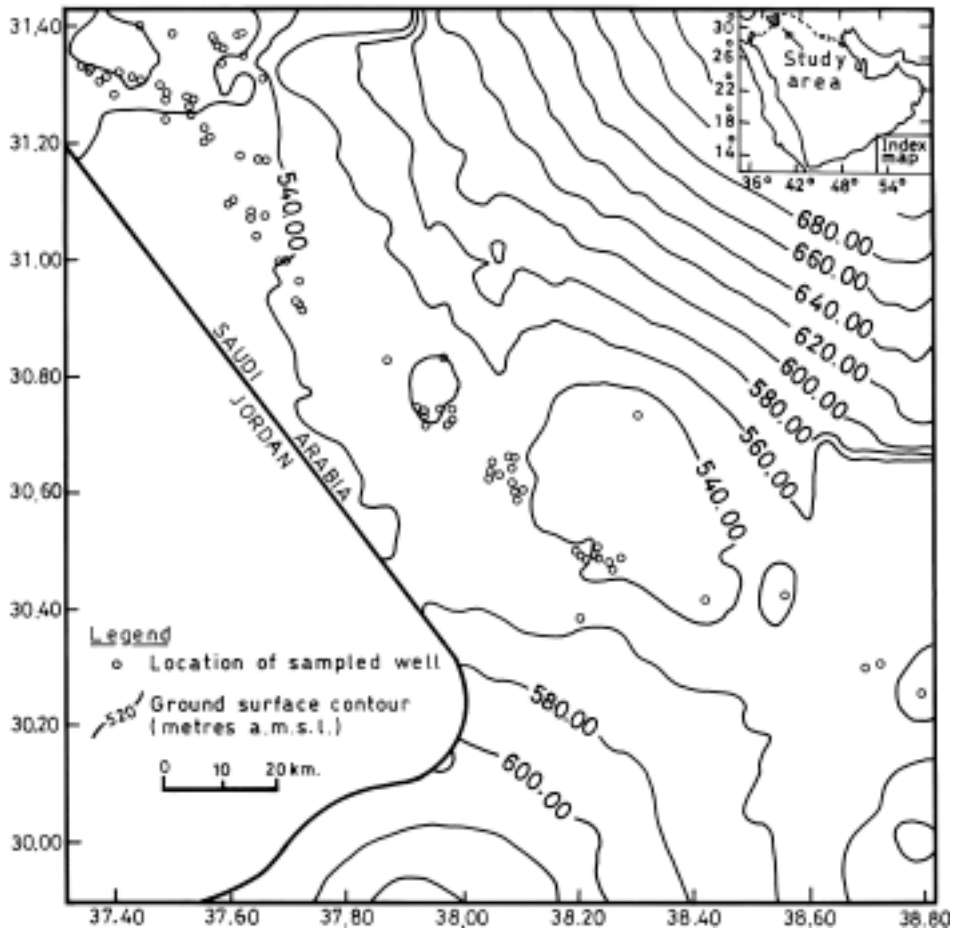


FIG. 1. Topographic map of the study area.

the southeast direction with a gradient of about 0.03 to reach 540 metres (a.m.s.l.), and from the south and southwest at about 640 metres (a.m.s.l.) towards a flat area of about 540 metres (a.m.s.l.) with a slope of 0.02. In this flat area lies an important topographic feature, the Sabkhat Hazouza. Sabkhat Hazouza is an exceedingly flat feature that covers a surface area of about 300 km<sup>2</sup> towards the center of the study area. It extends some 30 km in the north-west-southeast direction and its maximum width is about 15 km of an ellipsoidal form. The sabkhat is composed of layers and mixtures of sand, silt, mud and salts. Its surface is firm, and surrounded by sand dune that rise above the sabkhat surface. It is one of the inland sabkhat of the Arabian Peninsula (West *et al.*, 2000, Sabtan and Shehata, 2003, Al-Hurban and Gharib, 2004).

The area has been historically a pathway between Arabia, in the south, and the Sham region in the north. The population density is low due to the hyper arid conditions that prevail through most of the year. The total annual precipitation does not exceed 100 mm; the annual evaporation rates exceed 2000 mm. Groundwater has been obtained from Miocene and Pliocene sediments in the study area. These sediments are mainly interconnected sandstone, marl and limestone. Previous geological and hydrogeological studies that dealt with the study area are those of Powers *et al.* (1966), Smith (1980), Lozej (1983), and Bureau de Recherches Geologique et Minieres, BRGM (1985). The main purpose of this paper is to shed light on the occurrence of groundwater in these Miocene and Pliocene sediments and evaluate its water quality, water quality variations and the processes responsible for these variations. The relationship between these groundwaters and Sabkhat Hazouza will be addressed as well.

### Materials and Methods

An extensive field work has been carried out in the study area for a period of one month (March-April, 2003) during which a water well inventory of 229 wells tapping the Miocene and Pliocene sediments was executed, and geological and hydrogeological informations were collected. A global positioning system (GPS) Garmin 12 was used for location and elevation readings. This was supported with topographic sheets made available from the Saudi Survey Department. *In situ* measurements include pH, electrical conductivity (EC), temperature, identification and confirmation of the water-bearing layer being tapped. Eighty five samples were collected in plastic bottles after pumping the sampled wells for some 20 minutes. The samples were then further analysed in the laboratory for the determination of the major ions Ca<sup>2+</sup>, Na<sup>+</sup>, Mg<sup>2+</sup>, HCO<sub>3</sub><sup>-</sup>, SO<sub>4</sub><sup>2-</sup>, Cl<sup>-</sup>, in addition to TDS, SiO<sub>2</sub> and Fe. Standard methods were used (APH/AWWA/WPCF, 1989). Saturation indices were calculated with the help of PHREEQE computer program (Parkhurst and Appelo, 1999).

## General Geology

The main geological units building up the study area, from oldest to youngest, are shown on Fig. 2 :

- Tabuk Formation (Ordovician-Silurian),
- Limestone, chalk and marl (Eocene),
- Sandstone, marl and limestone (Miocene and Pliocene),
- Basalts (Tertiary-Quaternary),
- Sabkhah deposits (Quaternary-Recent),
- Eolian sand (Quaternary-Recent).

The Tabuk Formation outcrops at the southern west corner of the study area. It is buff, light brown to white, locally gray, yellow, red, and purple dark brown to black friable and strongly weathered, bedded sandstone with common quartz pebble zones and interbedded, thin, discontinuous shaly siltstone zones; ironstone concretion zones are found at several levels with abundant Tigillites. Micaceous shale with graptolitic zone at lower part of outcrop.

Limestone, chalk and marl of Eocene age outcrop in the northeast corner in the western part and in the southern limits of the study area. The Eocene consists of two members, an upper and a lower member. The lower member includes, cream, white and gray buff to tan weathering, chalky crystalline limestone with several nummulitic zones, tan to black nodular chert units, several silicious horizons and occasional calcite geodal zones. Dark chert residuum, limestone and other gravels cover part of the plain in the study area. The upper member consists of gray, white, tan to brown, massive, crystalline, commonly sandy limestone at top. Thin, white, chalk and marl with echinoids, and thin, gray, detrital fossiliferous limestone units occur in middle part. Gray to white, porous, chalky marl with a thin bluish clay bed and common iron sulphide concretions occur in lower part of this upper member.

Miocene and Pliocene outcrops occupy a band that extends from the southeast towards the northwest of central part of the study area (Fig. 2). It consists mainly of red, brown, and gray marly to calcareous sandstone with occasional conglomerate lenses; sandy marl with minor red sandy shale; white gray, and brown sandy limestone at top. In places, white to gray and creamy limestone grades up to calcareous sandstone with common small sandstone, limestone and shale pebbles and granules; locally resembles duricrust.

Basalt lava flows, regionally known as harrats, occupy the northwestern area. They rest unconformably over older units. These are formed of Olivine basalt with local thin aplite dikes; in places scoriaceous and vesicular. The harrats include as well bedded pyroclastics, plugs and cones. Thin lava fields discontinuously cover underlying rocks.

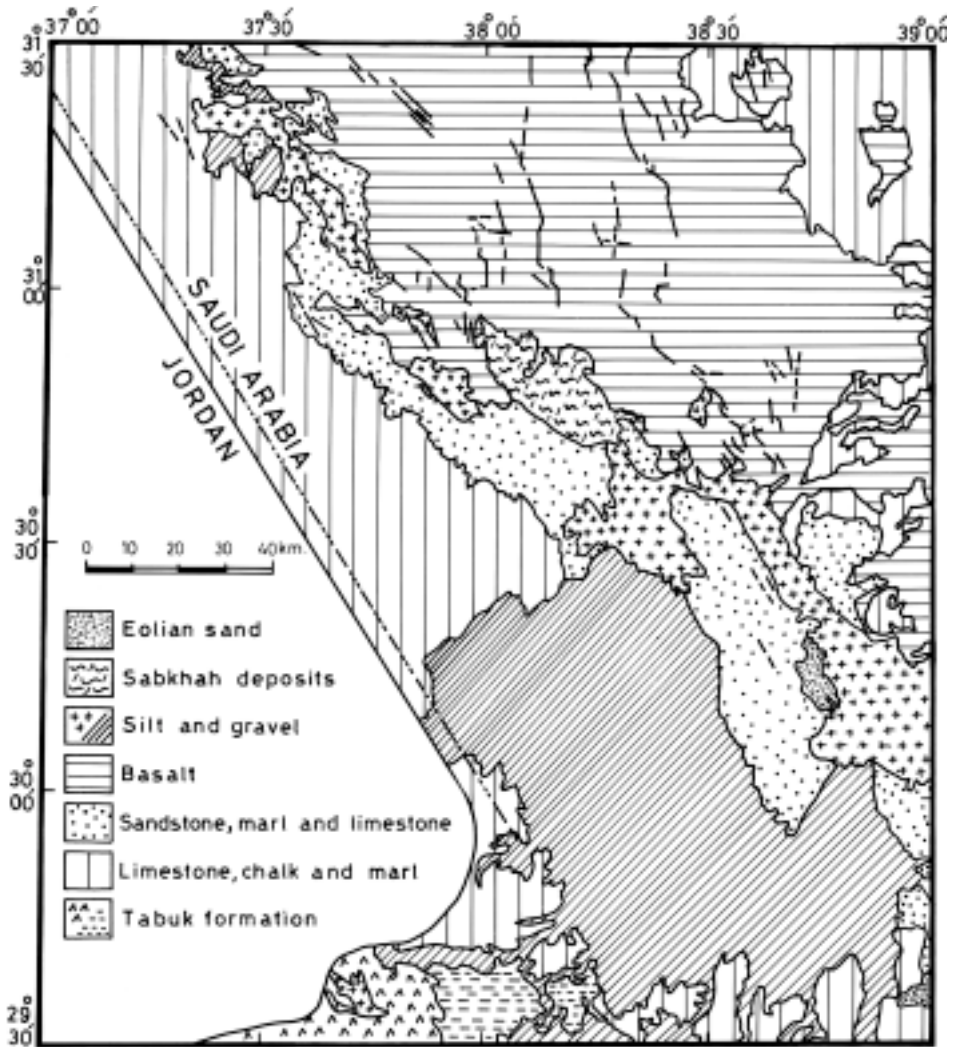


FIG. 2. Geological map of the study area.

Quaternary and recent deposits include three mappable units (Fig. 2). These are silt and gravel plains, sabkha deposits and eolian sand. The silt and associated sediments including caliche-like and gypsiferous deposits occur in depressions. Gravels of local origin make gravel plains, derived mainly from rocks of Eocene age. The Sabkha deposits consist of layers and mixtures of sand, silt, mud and salts. Sabkhas, in the study area, represent areas of equilibrium between aeolian sedimentation and deflation, controlled by the local water table. The water is necessarily higher than bedrock, and the base level of flatation lies just above the capillary fringe in the sediments above the water table. Evaporation through the surface causes the formation of brines and precipitation of evaporite minerals, mainly halite, gypsum and anhydrite. In places, a dry surface covered by few millimetres of wind blown sand occurs. Elsewhere silty material with scattered flakes of gypsum cover the ground surface in sabkhas. Eolian sand is mostly mobile sand dunes.

Structurally the study area can be considered a part of a basin that lies to the west of the Jauf arch. The uplift of this arch formed a horse which has been subjected to deeper erosion so that beds from the Devonian to the Late Tertiary have disappeared (BRGM, 1985). The sedimentary succession is clearly of a more open-marine environment containing finer sediments and carbonates. Main fault trend is NW-SE to NNW-SSE probably genetically linked to the rifting of the Red Sea and associated tectonics. Subsidence seems to have been caused by extensional forces in the crust. The latest developments in the study area are the sabkhas and the sand dunes. Sabkhas seem to date from humid phases than the present. The humid phases witnessed periods where recharge was accelerated; eolian cover masks extensive lacustrine deposits.

### **Groundwater Flow**

The groundwater level contour map of the Miocene-Pliocene aquifer system in the study area is shown on Fig. 3. The figure summarizes the distribution of the piezometric head. It varies from 510-600 m (a.m.s.l.). The general groundwater flow moves towards the whereabouts of Sabkhat Hazouza. There are three hydraulic gradients, one in the direction from northeast towards the sabkha with an average value of 0.003, a second flow directions comes from the south-southwest with an average hydraulic gradient of 0.001, and a third direction in the northwestern corner with a hydraulic gradient of about 0.0015.

The groundwater coming from the northeast is possibly attributed to the Tertiary-Quaternary basalts that outcrop in the area, and that coming from the south-southwest is associated with the outcrops of the Tabuk Formation. Within the Sabkhat Hazouza the subterranean flow gathers the water in a piezometric depression that also corresponds to a topographic depression, and as the water table is less than 2 metres deep high evaporation rates cause the concentration

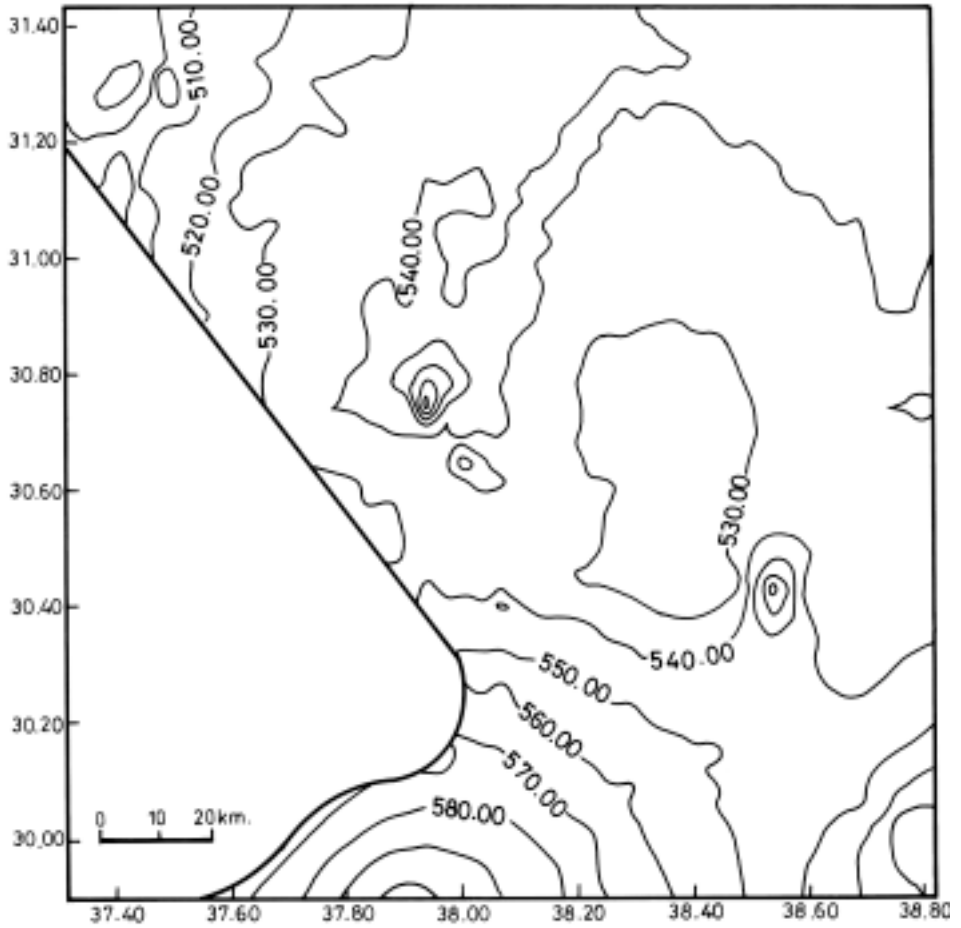


FIG. 3. Groundwater level contour map ( in a.m.s.l.).

of brine and evaporites close to the ground surface. Vertical recharge to the Miocene-Pliocene seems to be very restricted under the prevailing arid conditions. Restricted and limited recharge takes place in exceptional winter seasons when sleet forms on the ground surface. The main groundwater flow takes place as lateral groundwater flow. The average transmissivity of the Miocene-Pliocene aquifer system ranges between 20 m<sup>2</sup>/day and 170 m<sup>2</sup>/day; the average storativity varies from  $0.11 \times 10^{-2}$  to  $3.7 \times 10^{-2}$  (BRGM, 1985).

### Groundwater Quality

The groundwater quality within the Miocene-Pliocene of the study area varies from one place to another and exhibits wide range of values Table 1. The total dissolved (TDS) vary from 430 to 6000 mg/l. Values greater than 1500 mg/l were mainly encountered towards the center where Sabkhat Hazouza is formed.

TABLE 1. Summary statistics of the major ions concentration in the Miocene-Pliocene groundwater.

Constituent	Average	Minimum	Maximum
TDS (mg/l)	1650	430	6000
EC (μmhos/cm)	1900	700	8200
Na <sup>+</sup> (mg/l)	360	75	1820
Ca <sup>2+</sup> (mg/l)	180	15	3100
Mg <sup>2+</sup> (mg/l)	60	10	400
HCO <sub>3</sub> <sup>-</sup> (mg/l)	130	65	400
Cl <sup>-</sup> (mg/l)	620	110	2830
SO <sub>4</sub> <sup>2-</sup> (mg/l)	400	95	1170
SiO <sub>2</sub> (mg/l)	20	10	70
Fe <sup>2+</sup> (mg/l)	3	0	9

The anions relationships are as follows:

$$r \text{Cl}^- > r \text{SO}_4^{2-} > r \text{HCO}_3^-$$

the cations relationships are:

$$r \text{Na}^+ > r \text{Ca}^{++} > r \text{Mg}^{++} > r \text{K}^+$$

where r stands for milliequivalent per litre.

The X-Y relationship of sodium against chloride is shown on Fig. 4. The solid line on the graph represents a 1:1 relation while the dashed lines above



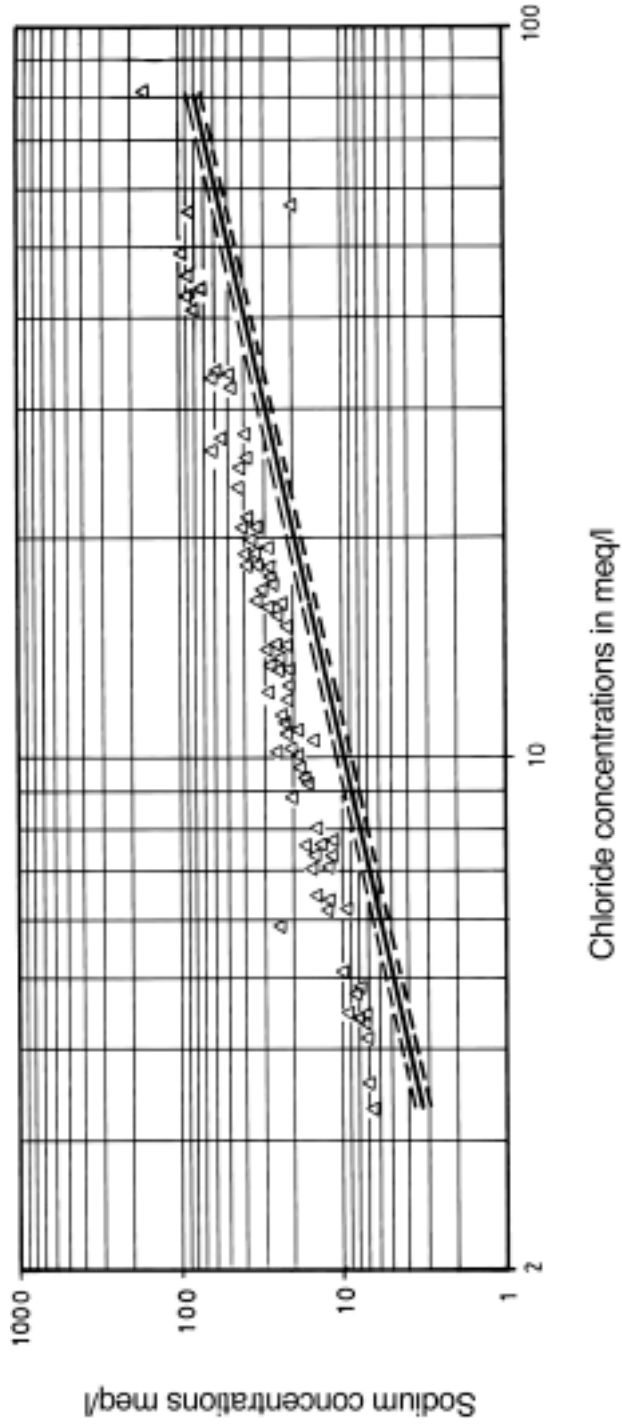


FIG. 4. X-Y relationship for sodium against chloride.

and below represent  $\pm 10\%$  difference plots. Almost all of the points except one sample the  $\text{Na}^+$  concentrations exceed the  $\text{Cl}^-$  concentrations. This increase in  $\text{Na}^+$  concentrations may have resulted from an ion-exchange process of incoming recharge water through lateral groundwater flow as explained above. The one-sample where the  $\text{Cl}^-$  concentration exceeds the  $\text{Na}^+$  concentrations could possibly be due to reverse ion-exchange process. The X-Y relationship of  $(\text{Ca}^{++} + \text{Mg}^{++})$  against  $(\text{HCO}_3^- + \text{SO}_4^-)$  is shown on Fig. 5. The solid line represents again a 1:1 relation while the dashed lines represent  $\pm 10\%$  difference plot. The majority of sample plots show that the concentrations of  $(\text{Ca}^{++} + \text{Mg}^{++})$  exceed the concentrations of  $(\text{HCO}_3^- + \text{SO}_4^-)$ . Very limited number of samples maintain a 1:1 relation; in few samples the concentration of  $(\text{HCO}_3^- + \text{SO}_4^-)$  exceeds that of  $(\text{Ca}^{++} + \text{Mg}^{++})$ . There seems to be several hydrochemical processes responsible for these relationships including ion-exchange, reduction of sulphates or combination of both processes. Most likely ion-exchange process seems to be the most dominant.

Table 2 summarizes calculated saturation indices for the minerals calcite, dolomite, gypsum, anhydrite and the dissolved carbon dioxide. All the samples are undersaturated with respect to gypsum and anhydrite, eight samples gave positive values for the saturation index of calcite and six showed positive values for the dolomite. The  $\text{Pco}_2$  has higher values than that of the atmosphere. All these results support that the process of mineral dissolution is active in the aquifer system, though with different rates.

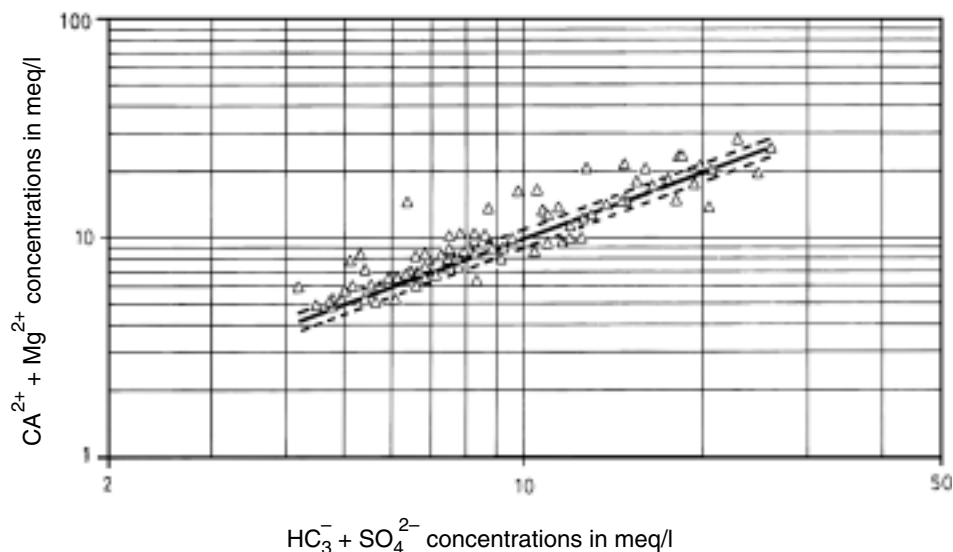


FIG. 5. X-Y relationship for  $(\text{Ca}^{2+} + \text{Mg}^{2+})$  against  $(\text{HCO}_3^- + \text{SO}_4^-)$ .

TABLE 2. Summer statistics for calculated saturation indices.

Statistics	Calcite _ SI	Dolomite _ SI	Gypsum _ SI	Anhydrite _ SI	CO2(g) _ SI
Mean	-0.365	-0.728	-1.144	-1.315	-1.914
Standard error	0.035	0.064	0.033	0.033	0.018
Median	-0.444	-0.873	-1.177	-1.348	-1.972
Standard deviation	0.323	0.589	0.305	0.305	0.166
Sample variance	0.104	0.347	0.093	0.093	0.027
Kurtosis	1.160	0.607	0.446	0.445	0.739
Skewness	0.710	0.666	0.594	0.594	1.130
Minimum	-1.248	-2.235	-1.766	-1.938	-2.161
Maximum	0.733	1.068	-0.195	-0.365	-1.395

### Major Ions Distribution

The spatial distributions of major ions concentrations in the Miocene-Pliocene groundwater of the study area are illustrated on Figs. 6 and 7. The distributions of sodium, calcium and magnesium ions show similar patterns. Sodium ion concentrations increase towards the northeast and north directions where it reaches values greater than 600 mg/l. Relatively high concentrations of more than 500 mg/l are also encountered towards the central western part of the study area. An ellipsoidal shape encircled by contour 200 mg/l is found towards the southern central part. A similar pattern of spatial distribution is exhibited by Calcium ion concentrations. Towards the north it is greater than 260 mg/l ; to the west it makes anomalies following the contour 200 mg/l; and towards the southern part it drops to less than 50 mg/l. The same picture is demonstrated by magnesium ion distribution. Highest values of magnesium reach some 80 mg/l and lowest values are indicated by contour 20 mg/l. The anions distributions are shown on figure. Chloride ion concentrations show an anomaly towards the central western segment of the study area, and towards the northwest corner. These anomalies are delineated by contour 900 mg/l. Relatively lower concentrations are encircled by contour 300 mg/l towards the south central part of the area. Sulphate ion concentrations reflect a different picture. It seem to be relatively higher toward the western and eastern segments of the study area. These two segments conform quite well with the geographical locations of the harats of the Tertiary-Quaternary basalts and the Eocene limestone, chalk and marl (Fig. 2) outcrops. The bicarbonate ion distribution is very different from all other ions concentrations. It is relatively high (240 mg/l) on the eastern and mid-eastern segments where the harrat basalts are exposed. It seems that recharge water of

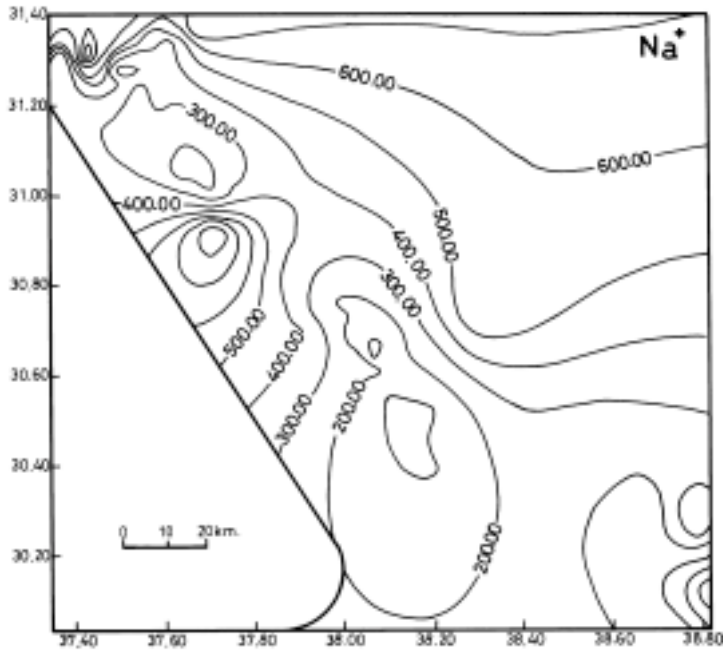


FIG. 6a. Areal distribution of dissolved sodium in groundwater (in mg/l).

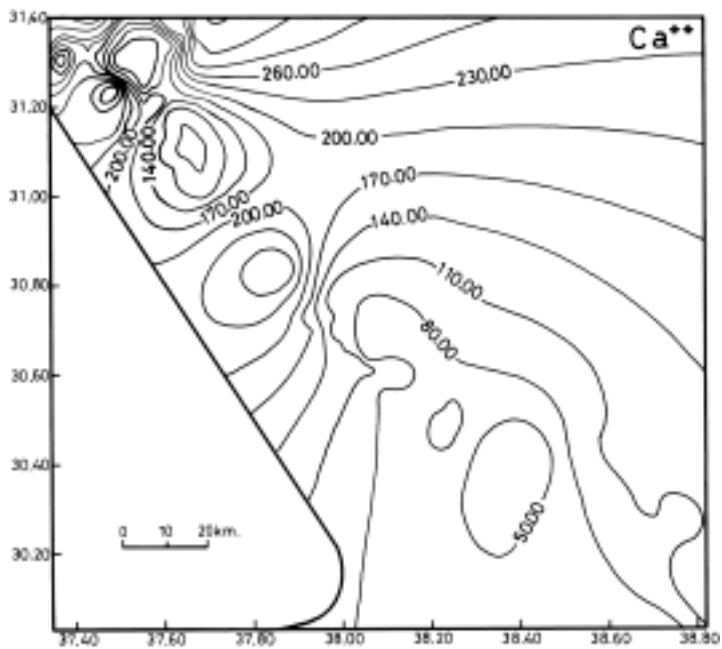


FIG. 6b. Areal distribution of dissolved calcium in groundwater (in mg/l).

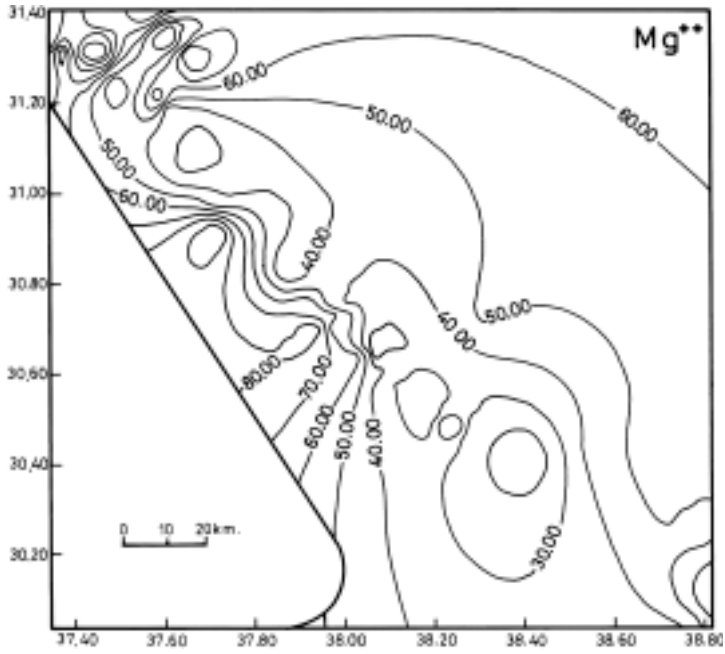


FIG. 6c. Areal distribution of dissolved magnesium in groundwater (in mg/l).

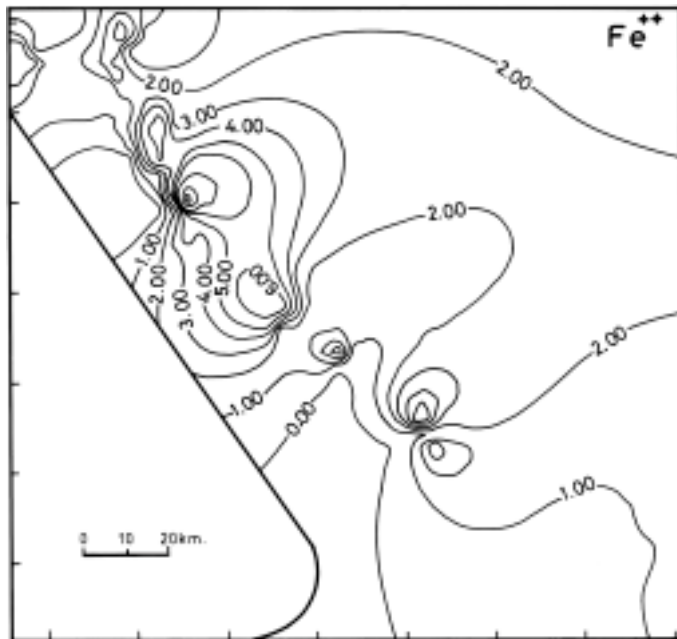


FIG. 6d. Areal distribution of dissolved iron in groundwater (in mg/l).

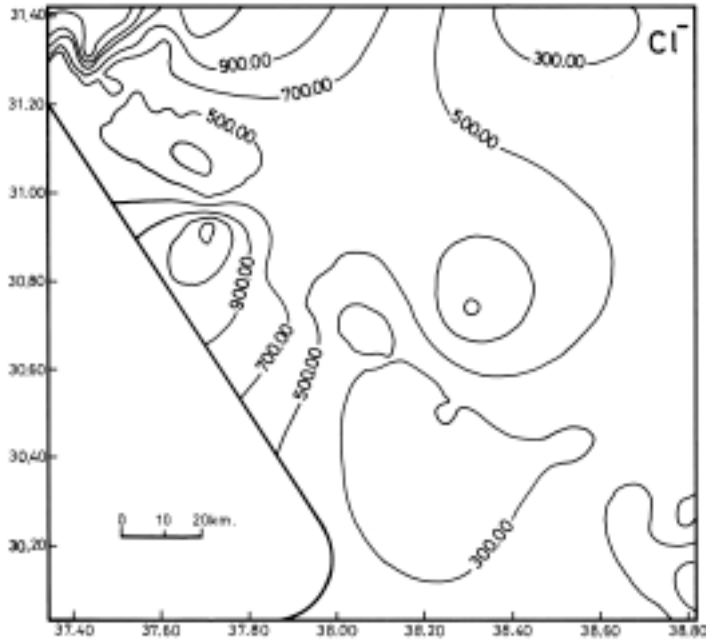


FIG. 7a. Areal distribution of dissolved chloride in groundwater (in mg/l).

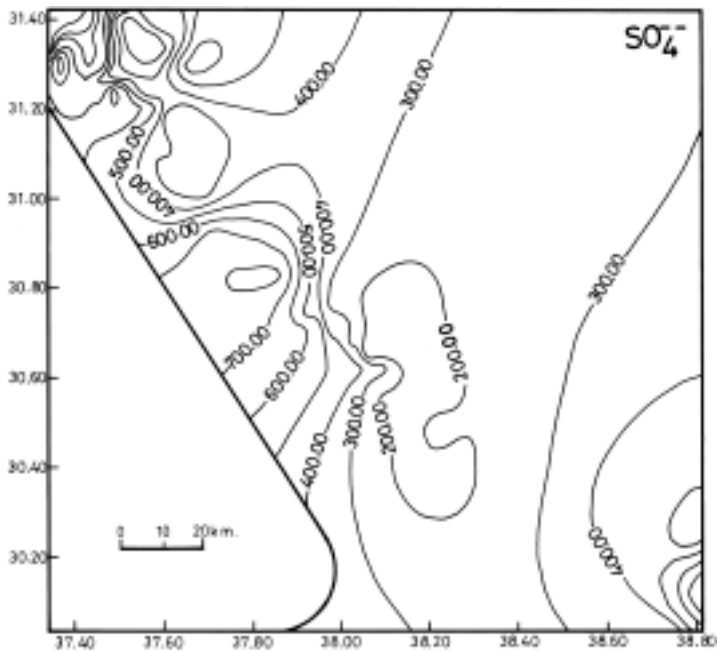


FIG. 7b. Areal distribution of dissolved sulphate in groundwater (in mg/l).

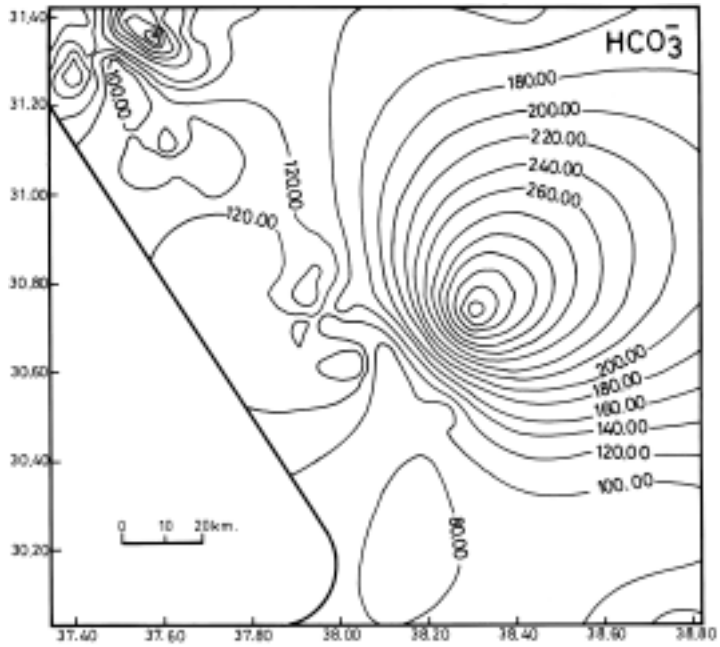


Fig. 7c. Areal distribution of dissolved bicarbonates in groundwater (in mg/l).

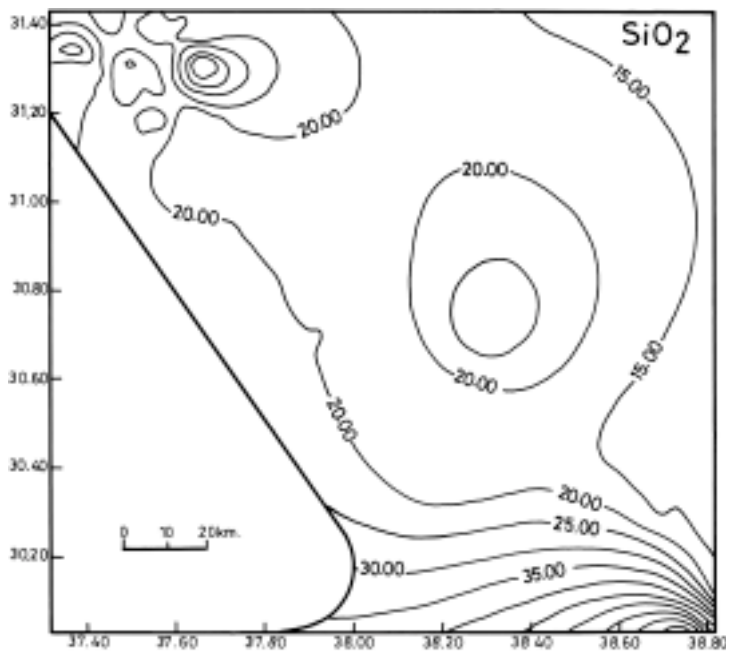


Fig. 7d. Areal distribution of dissolved silica in groundwater (in mg/l).

relatively higher bicarbonate concentrations comes through these fractured, vesicular, scorieous volcanic rocks, and, possibly through beds of the surface tributaries of the drainage system that flow towards Wadi As-Sirhan. The dissolved silica spatial distribution reflects variations and shows a sharp decrease from relatively higher concentrations in the southeast corner (35 mg/l) to some 15-20 mg/l on the average. An average concentration of dissolved iron distribution in the Miocene-Pliocene groundwater can be described as heterogeneous. Concentrations greater than 3 mg/l are restricted towards the western edge of the study area.

Based on the spatial distributions of the major ions, dissolved silica and dissolved iron in the Miocene-Pliocene groundwater, it seems that the concentration of salts in Sabkhat Hazouza is restricted to the very few meters close to the ground surface. These concentrations seem not to extend in depth within the Miocene-Pliocene groundwater chemistry. A possible chemical process in this regard is leaching. On the contrary the relatively lower anomalies of ionic concentrations are southward towards a shifted position from that of the sabkha.

### Hydrochemical Facies

The Durov diagram (Durov, 1948, Lloyd and Heathcote, 1985) was used to outline the hydrochemical water types and hydrochemical facies in the study area. The Durov plot (Al Bassam *et al.*, 1997) was also useful in detecting the chemical processes that took place in the aquifer. Figure 8 shows the Durov plot of the collected samples. The hydrochemical facies as deduced from this plot are, in order of abundance:

1.  $\text{Na}^+ \text{Cl}^-$  water type represent more than 50% of the collected water samples, fall in square 9.
2.  $\text{Cl}^-$  water type in square 8 and + has no dominant cation. This facies indicates limited reverse ion exchange within  $\text{CaCl}_2$  types.
3.  $\text{SO}_4^-$  and  $\text{Na}^+$  ions as being important and this indicates probably mixing influence of  $\text{CaSO}_4$  waters with  $\text{NaCl}$  waters, square 6.
4.  $\text{Ca}^{+2}$ ,  $\text{Mg}^{+2}$  ( $\text{HCO}_3^-$ )<sub>2</sub> ion with  $\text{Na}^+$  becoming more important. It is believed that this type is of recent recharge origin affected by ion-exchange, square (5 and 6).

The main hydrochemical processes seem to be involved on the evolution of the hydrochemical facies of the Miocene-Pliocene groundwater are simple mixing, ion-exchange and limited reverse ion exchange processes. Mixing has occurred between saline fossil water and relatively low salinity recharge water reaching the aquifer through fracture zones, vesicles within the basalts and possible collapse zones within the limestone, chalk and marl. Ion exchange



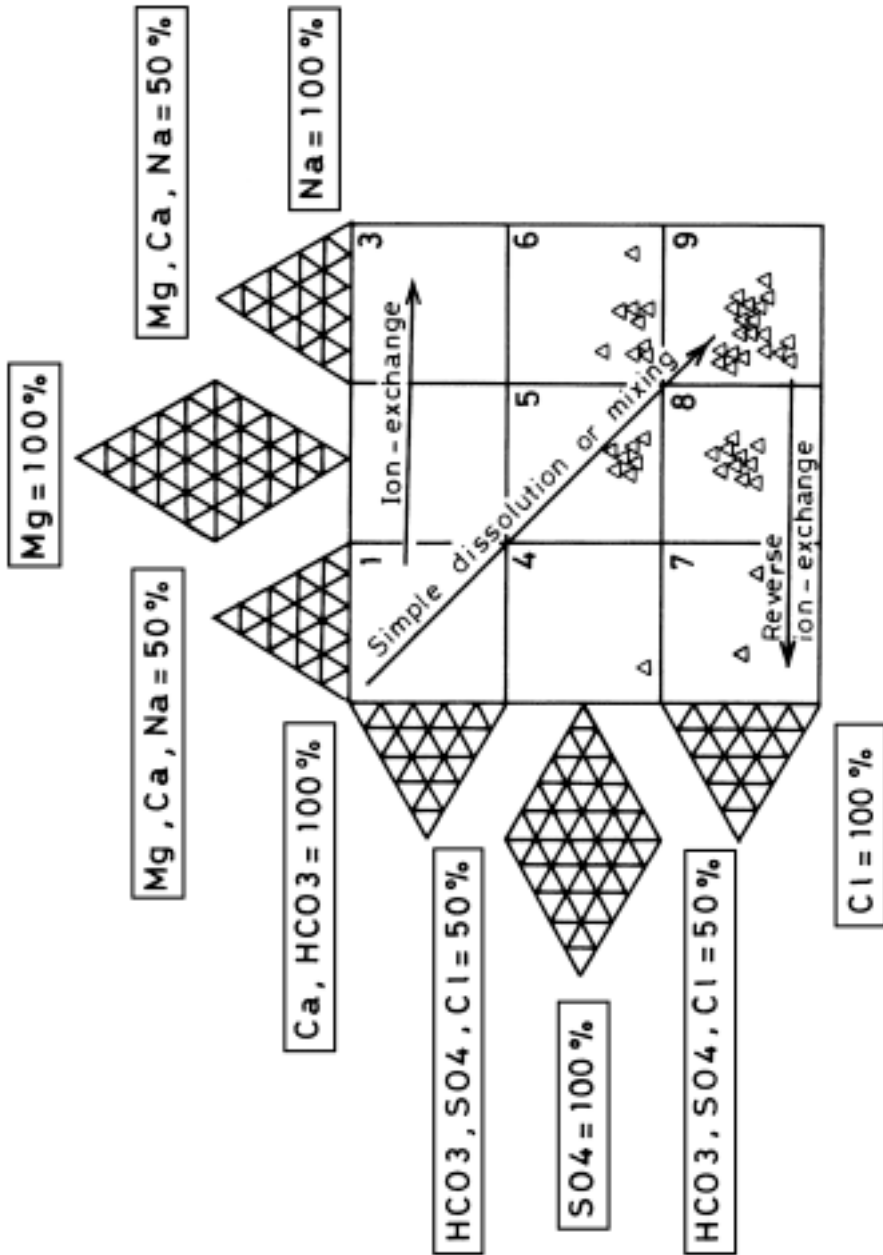


FIG. 8. Durov diagram for the major dissolved constituents.

reactions occurred within low salinity zone producing important amount of sodium. Reverse ion exchange reactions took place within sodium and calcium chloride types. In addition to these, leaching and simple dissolution of aquifer material and its matrix is also expected.

### Discussion and Conclusion

The Miocene-Pliocene aquifer system in northern Saudi Arabia represents an important water resource in this hyper arid part of the world. Groundwater is found within a heterogeneous layering system of sandstone, marl and limestone. It moves towards a central depression in Wadi As Sirhan in the whereabouts of Sabkhat Hazouza, under hydraulic gradient of 0.001 to 0.003. Average transmissivity ranges in the system between 20 m<sup>2</sup>/day and 170 m<sup>2</sup>/day; average storativity varies from  $0.11 \times 10^{-2}$  to  $3.7 \times 10^{-2}$ . The TDS values range between 430 and 6000 mg/l. Na<sup>+</sup> and Cl<sup>-</sup> ions are the most dominant in groundwater with Ca<sup>2+</sup> and SO<sub>4</sub><sup>-2</sup> ions as being next in importance. More than 50% of the collected water samples are of NaCl water type, Ca<sup>+2</sup>-Mg<sup>+2</sup>-SO<sub>4</sub><sup>-2</sup> ions in Na<sup>+</sup> Cl<sup>-</sup> represent a mixture of calcium sulphate waters with sodium chloride water. The main hydrochemical processes for the groundwater quality are ion exchange, mineral dissolution, simple mixing in addition to reverse ions exchange processes. Recent recharge is restricted to the harrat basalts in the eastern segment of the study area. Other parts receive lateral groundwater flow. The spatial distribution of the major ions, dissolved silica and iron within the Miocene-Pliocene aquifer seems to be independent of Sabkhat Hazouza. The salt concentrations within the sabkhat is restricted to the very few meters close the ground surface. Leaching is an active process under such conditions.

### Acknowledgement

The author would like to express his thanks and gratitude to Mr. Hussein Alfifi for his help with the computer work and to Mr. Aftab Aziz for drawing the figures and typing the manuscript.

### References

- Al-Bassam, A.M., Awad, H.S. and Al-Alawi, J.A. (1977) Durov Plot: A Computer Program for Processing and Plotting Hydrochemical Data, *Groundwater*, **35**(2): 362-367.
- Al-Hurban, A. and Gharib, I. (2004) Geomorphological and sedimentological characteristics of coastal and inland sabkhas, Southern Kuwait, *Journal of Arid Environments*, **58**: 59-85.
- APH/AWWA/WPCF (1989) *Standard Methods for the Examination of Water Wastewater*, Washington, DC, American Public Health Association.
- Bureau de Recherches Geologiques et Minières (BRGM) (1985) *Water, Agriculture, and Soil Studies of the Saq and Overlying Aquifers*, Unpub. Report, Ministry of Agriculture and Water, Riyadh, Kingdom of Saudi Arabia.

- Durov, S.A.** (1948) Natural waters and graphic representation of their composition, *Dokl. Akad. Nauk SSSR*, **59**: 87-90.
- Lloyd, J.W. and Heathcote** (1985) *Natural Inorganic Chemistry in Relation to Groundwater*, Clarendon Press, Oxford, 296 p.
- Lozej, G.P.** (1983) *Geological and Geochemical Reconnaissance Exploration of the Cover Rocks in Northwestern Hijaz - Initial Results and Recommendations*, Open File Report RF-OF-03-2. Directorate General of Mineral Resources, Jeddah, Saudi Arabia.
- Parkhurst, D.L. and Appelo, C.A.J.** (1999) *User's Guide to PHREEQC (Version 2) – A Computer Program for Speciation, Batch-Reaction, One-Dimensional Transport and Inverse Geochemical Calculations*, U.S. Geological Survey Water Resources Investigation Report, 99-4529, 314 p.
- Powers, R.W., Rameriz, L.F., Redmond, C.D. and Elberge, E.L.** (1966) *Geology of the Arabian Peninsula: Sedimentary Geology of Saudi Arabia*, United States Geological Survey, Professional Paper, **560-D**, 147 p.
- Sabtan, A.A. and Shehata, W.M.** (2003) Hydrogeology of Al-Lith Sabkha, Saudi Arabia, *Journal of Asian Earth Sciences*, **21**: 423-429.
- Smith, L.C.** (1980) *Brines of Wadi as Sirhan of Saudi Arabia*, United States Geological Survey Technical Report 1.
- West, I.M., Lashhab, M.I. and Muhan, I.M.** (2000) North African sabkhas and lagoons compared to those of the Arabian Gulf, *Proceedings of the Sixth Mediterranean Petroleum Conference, an Exhibition, November 23-25<sup>th</sup>, 1999, Libya (G.S.P.L.A.J.)*, 845 p.

## تقييم هيدروكيميائي لنظام الخزانات الجوفية ميوسين - بليوسين في شمال المملكة العربية السعودية

عبد العزيز محمد البسام

قسم الجيولوجيا ، كلية العلوم ، جامعة الملك سعود

الرياض - المملكة العربية السعودية

Email: ambassam@ksu.edu.sa

المستخلص. يمثل نظام الخزانات الجوفية ميوسين - بليوسين مصدراً مهماً للمياه في شمال المملكة العربية السعودية. توجد المياه في نطاقات حاملة للمياه متعددة الطبقات من الحجر الرملي والطباشير والمارل. تتحرك المياه نحو سبخة حضوضه تحت تأثير معامل مائي بمعدل عام يساوي ٠,٠٠٢, يبلغ معدل معامل التوصيل المائي حوالي ٢٠-١٧٠ م<sup>٢</sup>/يوم، كما يبلغ معدل معامل التخزين لهذه الطبقات حوالي ١١, ٠ × ١٠<sup>-٢</sup> - ٧, ٣ × ١٠<sup>-٢</sup> تتراوح تراكيز الأملاح الذاتية في المياه الجوفية بين ٤٣٠-٦٠٠ مليجرام/ لتر. يمثل كلوريد الصوديوم النوع السائد للمياه (أعلى تراكيز للأملاح هي كلوريد الصوديوم) كما يأتي الكالسيوم والمغنسيوم والكبريتات في المرتبة التي تليه. تعتبر العمليات الهيدروكيميائية: التبادل الأيوني والإذابة والامتزاج وبصورة محدودة التبادل الأيوني العكسي هي المسؤولة عن الاختلافات في تراكيز الأملاح الذاتية. أشارت هذه الدراسة إلى أن التوزيع المكاني للعناصر الرئيسية والسيليكا والحديد المذابة في الماء لا ترتبط أو تعتمد على وجود سبخة حضوضه. وينحصر تأثير أملاح السبخة من الأمطار القليلة العلوية في المياه السطحية.